

The role of phosphorylation and dephosphorylation of shell matrix proteins in shell formation: an in vivo and in vitro study

Jinzhe Du^{1,4}, Guangrui Xu^{3,4}, Chuang Liu^{2,3*}, Rongqing Zhang^{1,3*}

¹ Institute of Marine Biotechnology, School of Life Sciences, Tsinghua University,
Beijing 100084 China

²Department of Biomaterials, Max Planck Institute of Colloids and Interfaces, Potsdam
14476, Germany

³ Department of Biotechnology and Biomedicine, Yangtze Delta Region Institute of
Tsinghua University, Jiaxing, Zhejiang Province, 314006, China

⁴These authors contributed equally.

E-mail: Chuang.Liu@mpikg.mpg.de (C.L);

rqzhanglab@mail.tsinghua.edu.cn (Q.Z)

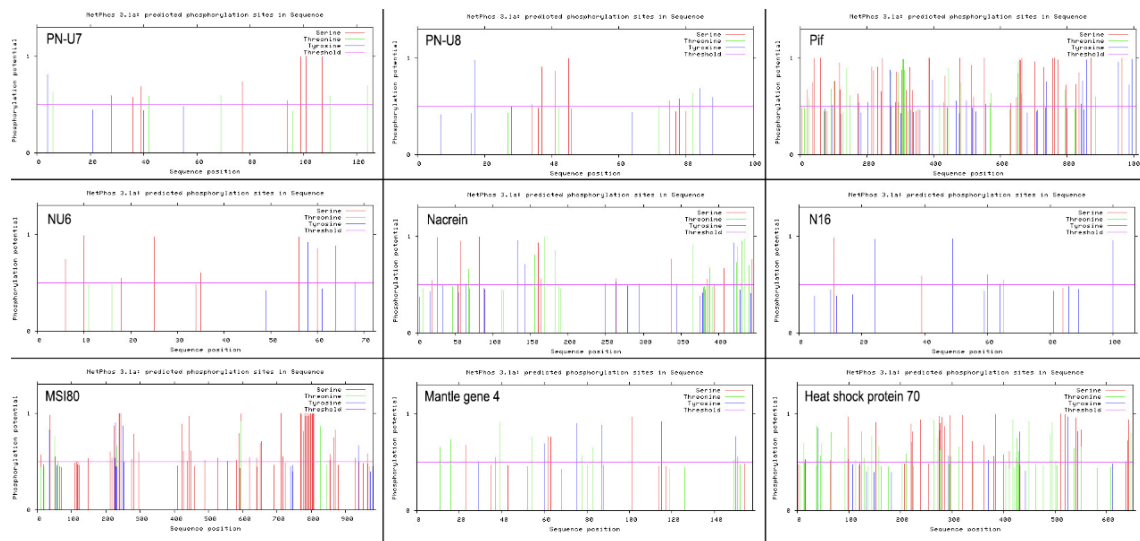


Figure S1. Prediction of phosphorylation sites of nine typical SMPs by NetPhos 3.1 Server. The phosphorylation sites of these proteins (Nacrein, N16, Pif, Mantle gene 4, Heat shock protein 70, PNU7, PNU8, NU6 and MSI80) were presented. Phosphorylation potential above 50% was confidential.

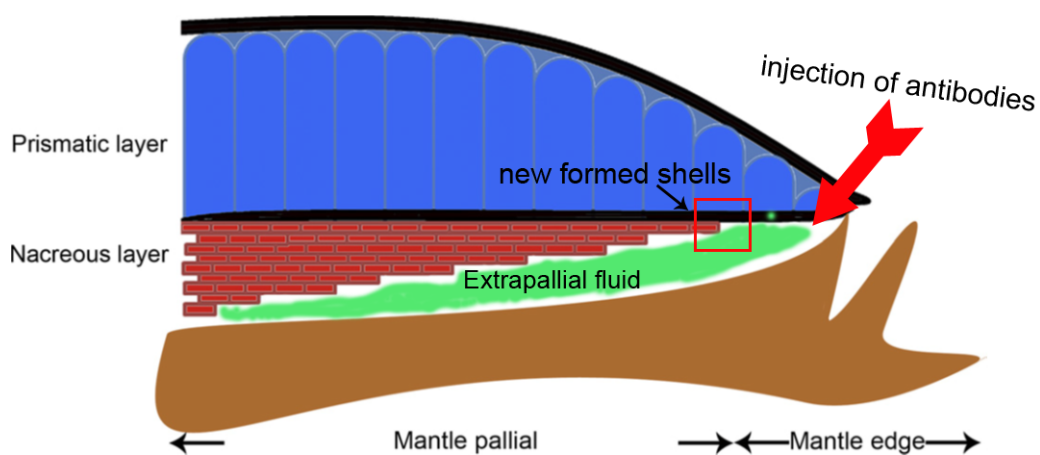


Figure S2. Diagram of injection of antibodies into extrapallial fluid and the new formed shells of *P. fucata*.

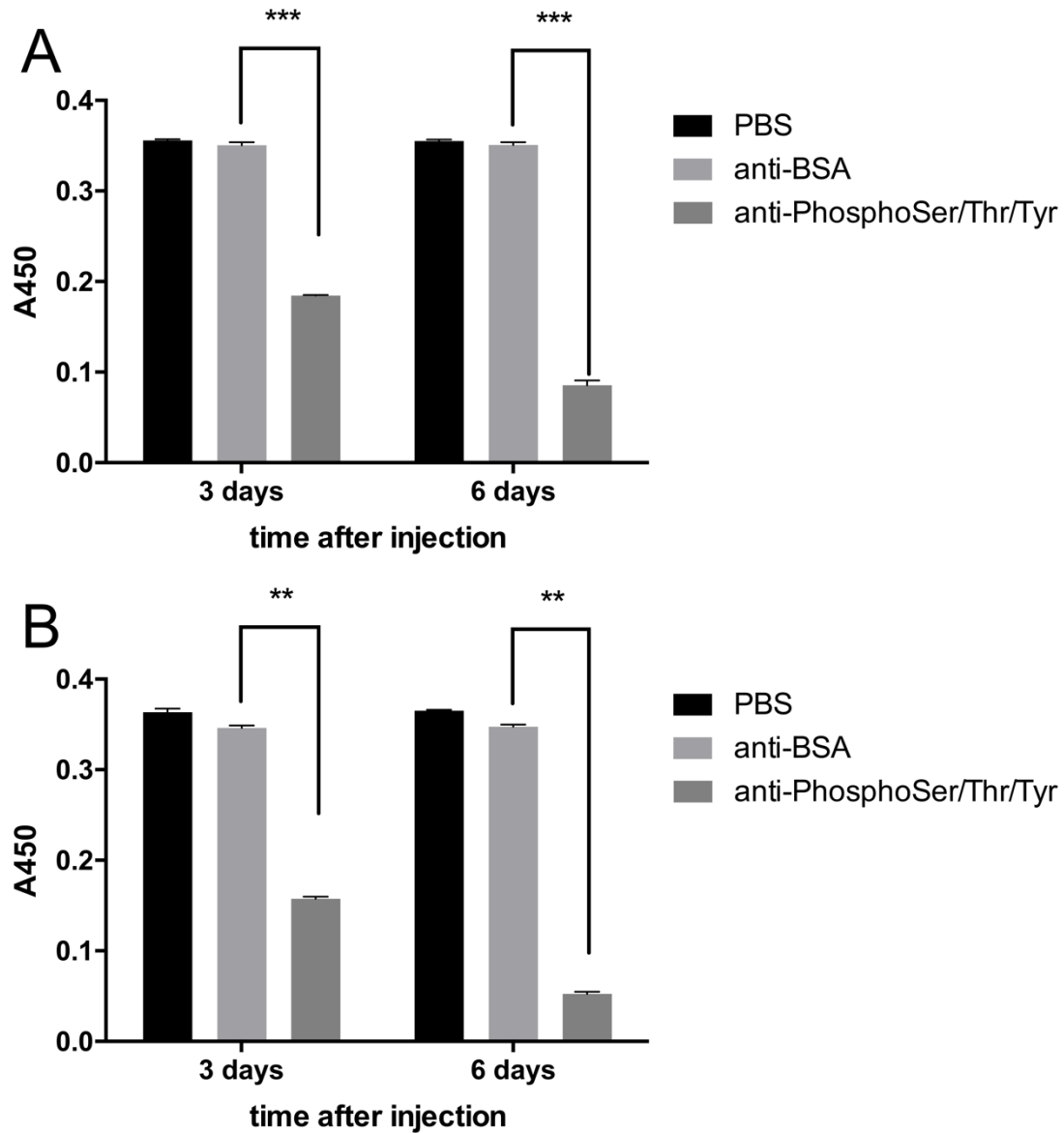


Figure S3. Detection of phosphorylation of extrapallial fluid proteins by ELISA. The A450 absorbance values were positively proportional to the phosphorylation extent of extrapallial fluid proteins in normal groups (A) and notching groups (B). The stars represented that there was significant difference (** $p < 0.001$, analyzed by multiple T-test) between anti-phosphoserine/threonine/tyrosine injected group and anti-BSA injected group after injection for 3 days and 6 days. And there was no significant difference between anti-BSA injected group and PBS injected group.

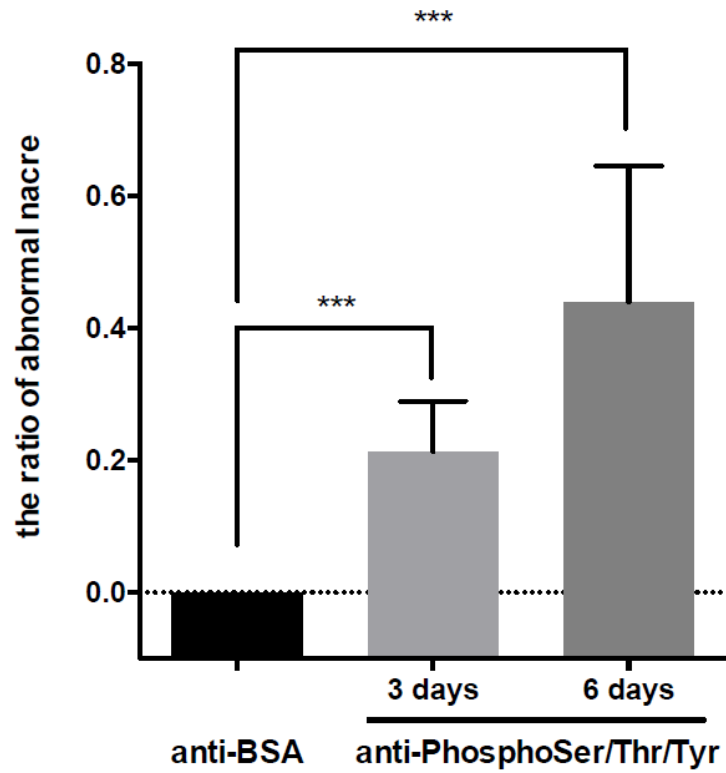


Figure S4. Comparison of the ratio of abnormal nacre to the whole nacre. The abnormal nacre was the overgrowth crystals in nacre tablets marked by red arrows (8F, 8H). The ratio of abnormal nacre to the whole nacre in anti-phosphoserine/threonine/tyrosine injected group after 3 days and 6 days were significantly higher (** $p < 0.001$, analyzed by multiple T-test) than anti-BSA injected group.

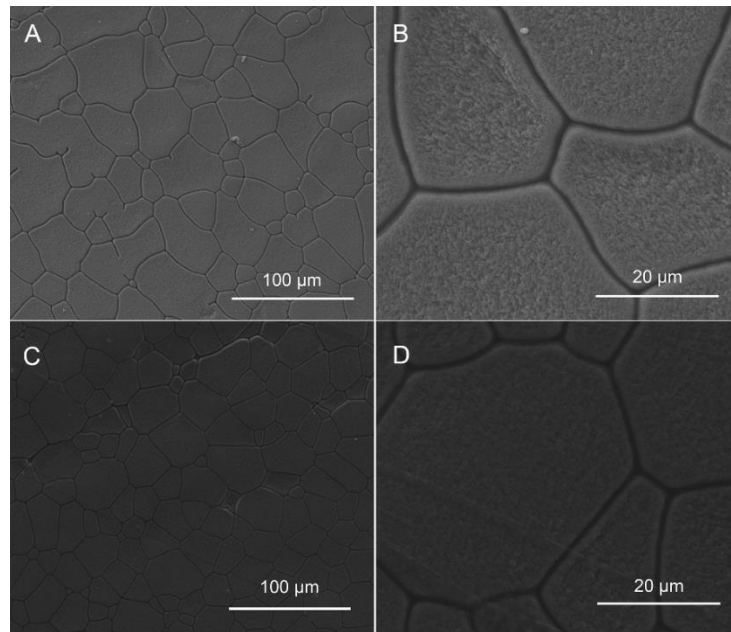


Figure S5. The SEM images of regenerated shells after shell notching. The SEM images of newly formed shells of anti-phosphoserine/threonine/tyrosine injected oysters (A, B) and anti-BSA injected oysters (C, D) were taken.

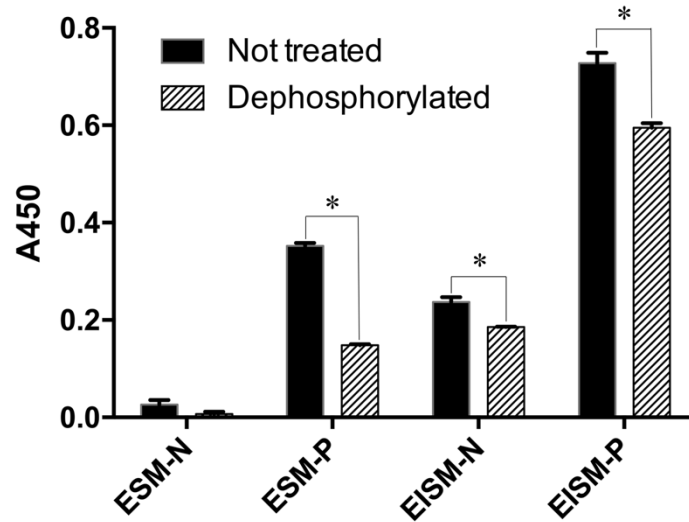


Figure S6. Detection of phosphorylation of shell matrix proteins (SMPs) by ELISA. The black dot meant untreated SMPs and the shaded dot meant dephosphorylated (DP) SMPs. From left to right were four SMPs (ESM-N, ESM-P, EISM-N and EISM-P). The A450 absorbance values were positively proportional to the phosphorylation extent. The stars represented that there was significant difference ($*p < 0.05$, analyzed by one-way ANOVA) between dephosphorylated and untreated SMPs. ESM-P/N: EDTA soluble matrix of prism/nacre; EISM-P/N: EDTA insoluble matrix of prism/nacre.

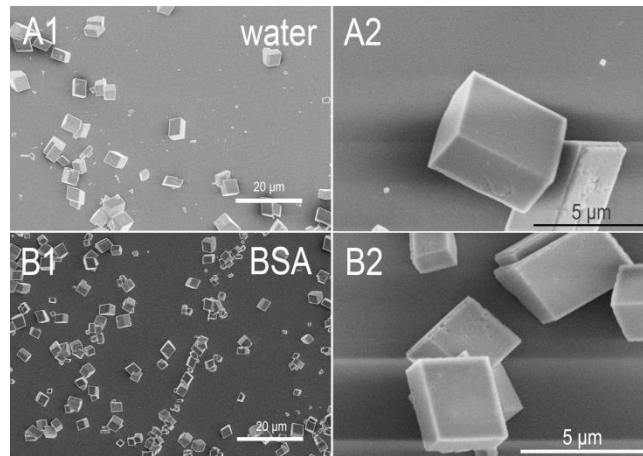


Figure S7. The effects of water and BSA on the morphology of calcium carbonate observed by SEM. Calcium carbonate crystals formed in the presence of water (A1 and A2) and 20 $\mu\text{g/mL}$ BSA (B1 and B2).

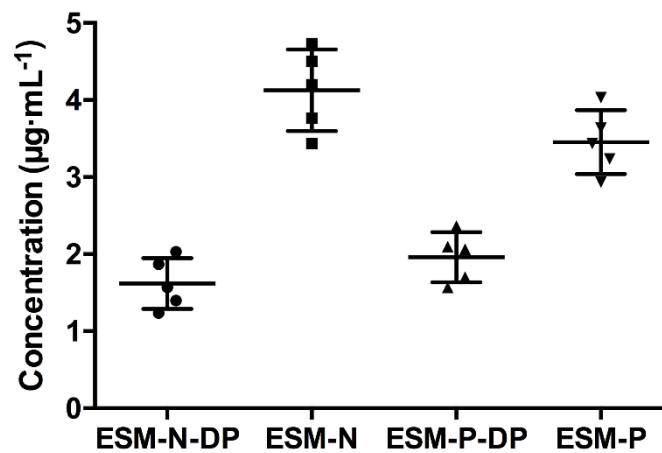


Figure S8. The amount of proteins occluded in the calcite. The crystals were first washed by DI water for three times and then were dissolved in the 0.5 M EDTA. The dissolved solution containing occluded proteins were concentrated by acetone for 1 h on ice. The solution was centrifugated at 4 $^{\circ}\text{C}$ and precipitated proteins were obtained. Finally, PBS buffer were added to dissolve proteins and the concentration were measured by Nanodrop 2000. Five independent experiment were conducted.